PHYSICAL REVIEW B VOLUME 54, NUMBER 22 1 DECEMBER 1996-II

# $I$-$V$ characteristics of Josephson-coupled layered superconductors with longitudinal plasma excitations

T. Koyama
*Institute for Materials Research, Tohoku University, Katahira 2-1-1, Aoba-ku, Sendai 980-77, Japan*

M. Tachiki
*National Research Institute for Metals, Sengen 1-2-1, Tsukuba 305, Japan*

(Received 10 June 1996)

Coupled equations for the interlayer phase differences in Josephson-coupled layered superconductors are derived in both current-biased and voltage-biased cases. These equations have a solution corresponding to the longitudinal Josephson plasma propagating along the $c$ axis. Using the numerical solutions for the systems composed of 100 junctions, we calculate the $I$-$V$ characteristics of the Josephson-coupled layered superconductors in the absence of an external magnetic field. Various types of $I$-$V$ characteristics reflecting the dynamics of the phase differences are obtained. [S0163-1829(96)06846-4]

## I. INTRODUCTION

It is widely believed that the superconducting layers in high-$T_c$ superconductors with large anisotropy are coupled by the Josephson effect. Several experimental results show the existence of the intrinsic Josephson effects in single crystals of high-$T_c$ superconductors.[1–8] For example it has been reported that the $I$-$V$ characteristics along the $c$ axis of Bi-2212 in the superconducting state are those expected in a Josephson-junction array.[2,4] The Fraunhofer pattern in the field dependence of the critical current has also been observed in those superconductors in a magnetic field parallel to the layers.[1] Recently, Matsuda *et al.*[7] observed a sharp resonance peak in microwave absorption experiments in single crystals of Bi-2212. This resonance peak has been identified with the Josephson plasma mode. These experimental results indicates that the electromagnetic properties of high-$T_c$ superconductors are well understood on the basis of a model assuming one-dimensional (1D) Josephson-junction array formed by superconducting layers of atomic-scale thickness. The mixed state of high-$T_c$ superconductors has been intensively studied on the basis of such a Josephson-coupled layered model.[9]

In this paper we investigate the $I$-$V$ characteristics of a 1D series of Josephson junctions to elucidate the intrinsic Josephson effects in high-$T_c$ cuprate superconductors. The equation for the phase differences in a Josephson-junction array is usually derived from the RSJ model.[10] The static and dynamical properties of 2D networks of conventional Josephson junctions have been investigated so far on the basis of the equation derived from the RSJ model.[11] However, as easily shown, in the case of a 1D series of Josephson junctions the equation obtained from the RSJ model fails to describe the interaction between the interlayer phase differences in the absence of an external magnetic field, that is, the junctions in a 1D array behave independently of one another in the simple RSJ model. To incorporate the interference effect among the junctions several equivalent circuits including a shunted impedance connected to an array of the circuits for the RSJ model have been proposed.[12] The phase locking or the synchronization of the voltage observed in conventional multijunction systems has been analyzed on the basis of those equivalent circuits.[12–14] However, the microscopic origin of the impedance which induces the coupling among the junctions is not clearly specified in those phenomenological models. In this paper we, therefore, first examine the dynamics of the phase differences in a 1D array of Josephson junctions and clarify the origin of the coupling between the interlayer phase differences in intrinsic layered superconductors. It is shown that the charging effect of the superconducting layers cannot be neglected in the systems composed of superconducting layers of atomic-scale thickness such as high-$T_c$ superconductors[15] and it induces the coupling between the interlayer phase differences.

The equation for the interlayer phase differences in intrinsic layered superconductors in the static case is derived from the Lawrence-Doniach model[16] and the Maxwell equations in the limit where the spatial variation of the amplitude of the order parameter is neglected.[17,18] The extension of the equation to the dynamical case is seen in Refs. 19 and 20. The equation for the phase differences derived in Ref. 19 neglects the effect arising from the charging of the superconducting layers. Thus the equation given in Ref. 19 is not applicable to the systems such as high-$T_c$ superconductors. The charging effect of the superconducting layers is incorporated in the equation for the phase differences derived in Ref. 20. However, the equation does not give the correct dispersion of the Josephson plasma mode in the Meissner state.[21] This fact indicates that the time-dependent part of the equation is incomplete. In this paper we improve the derivation of the dynamical equation for the interlayer phase differences in the absence of an external magnetic field and propose a new time-dependent equation in which the effect of the charging of the superconducting layers is properly taken into account within a classical theory in the presence of a transport current. The longitudinal Josephson plasma propagating along the $c$ axis can be correctly described by this equation. The equation for the phase differences is solved numerically in finite systems with 100 junctions in the current-biased and voltage-biased cases both to simulate the $I$-$V$ characteristics

0163-1829/96/54(22)/16183(9)/$10.00  © 1996 The American Physical Society

of Josephson junction arrays. The boundary effect between the outermost superconducting layers and the electrodes is incorporated in the calculations. The motion of the gauge-invariant phase differences shows complex behavior, depending on the material parameters and also on an applied current or voltage. The $I$-$V$ characteristics reflect sensitively the dynamics of the gauge-invariant phase differences. Various patterns of the $I$-$V$ characteristics are predicted.

## II. FORMULATION

Consider a layered superconductor in which the layers are coupled by the Josephson effect. We assume that the superconducting layers are extremely thin, so that the spatial variation of the phase and the electromagnetic field inside the layers may be neglected in the direction perpendicular to the layers. It is also assumed that the phase difference between the layers is uniform along the layers in the absence of an external magnetic field. In this case the total tunneling current between $(l+1)$th and $l$th layers, $J_{l+1,l}(t)$, is given by the sum of a pair current and a quasiparticle current in the presence of an electric field, $E_{l+1,l}(t)$, as follows:

$$J_{l+1,l}(t)=j_c \sin P_{l+1,l}(t)=\sigma E_{l+1,l}(t), \tag{1}$$

where $j_c$ and $\sigma$ are, respectively, the critical current density and the conductivity of the quasiparticle current, and $P_{l+1,l}(t)$ is the gauge-invariant phase difference between $(l+1)$th and $l$th layers defined by

$$P_{l+1,l}(t)\equiv\varphi_{l+1}(t)-\varphi_l(t)-\frac{2\pi}{\phi_0}\int_{z_l+s/2}^{z_{l+1}-s/2}dz\ A_z(z,t). \tag{2}$$

In the above equation $\varphi_l(t)$ is the phase of the order parameter on $l$th layer, $\phi_0$ is the unit flux $(hc/2e)$, and $z_l=l(D+s)$, $s$ and $D$ being the widths of, respectively, the superconducting and block layers.

Let us now derive the equation for $P_{l+1,l}(t)$ under the condition that a bias current is applied along the $c$ axis. From the current conservation law it follows

$$J_{l+1,l}(t)=J_{l,l-1}(t)-s\partial_t\rho_l(t), \tag{3}$$

in the present layered system, where $\rho_l(t)$ is the charge density on $l$th layer. Since the Maxwell equation $(\nabla\cdot\epsilon\mathbf{E}=4\pi\rho)$ gives the following relation in the present discrete case:

$$E_{l+1,l}(t)-E_{l,l-1}(t)=\frac{4\pi s}{\epsilon}\rho_l(t), \tag{4}$$

with $\epsilon$ being the dielectric constant of the block layers, we have the equation from Eqs. (3) and (4),

$$J_{l+1,l}(t)+\frac{\epsilon}{4\pi}\partial_t E_{l+1,l}(t)=J_{l,l-1}(t)+\frac{\epsilon}{4\pi}\partial_t E_{l,l-1}(t). \tag{5}$$

This equation indicates that the total current including the displacement current is conserved in each junction. From this observation we assume that the total current is equal to the current $I(t)$ supplied from an external current source,

$$j_c \sin P_{l+1,l}(t)+\sigma E_{l+1,l}(t)+\frac{\epsilon}{4\pi}\partial_t E_{l+1,l}(t)=I(t). \tag{6}$$

Note that this equation is similar to that in a single junction system in the RSJ model.[10] From this result we notice that the junctions in the present series are independent of one another, i.e., no interference effect takes place among the junctions, if we assume the usual *local* Josephson relation between the phase and the voltage, $V_{l+1,l}(t)=DE_{l+1,l}(t)$,

$$\partial_t P_{l+1,l}(t)=\frac{2e}{\hbar}V_{l+1,l}(t)=\frac{2\pi c}{\phi_0}DE_{l+1,l}(t). \tag{7}$$

However, as discussed in Refs. 22 and 23 the above relation is not valid in systems in which the charging effect cannot be neglected. In systems composed of microscopic series of the Josephson junctions as in the case of high-$T_c$ cuprates Eq. (7) should be modified as seen in the following. Taking the time derivative of Eq. (2), we have the relation

$$\frac{\phi_0}{2\pi c}\partial_t P_{l+1,l}(t)=\left[A_0(z_{l+1},t)+\frac{\phi_0}{2\pi c}\partial_t\varphi_{l+1}(t)\right]-\left[A_0(z_l,t)+\frac{\phi_0}{2\pi c}\partial_t\varphi_l(t)\right]+V_{l+1,l}(t), \tag{8}$$

where $A_0(z,t)$ is the scaler potential. It is noted that the first and second terms on the right-hand side of Eq. (8) is related to the charge density on $(l+1)$th and $l$th layers, respectively. Then we assume the following relation between the charge density and the scaler potential:[23–25]

$$\rho_l(t)=-\frac{1}{4\pi\mu^2}\left[A_0(z_l,t)+\frac{\phi_0}{2\pi c}\partial_t\varphi_l(t)\right], \tag{9}$$

where $\mu$ is the Debey length of the superconducting charge, which is usually much shorter than the London penetration depth $(\mu\ll\lambda_L)$. Substituting Eq. (9) into Eq. (8) and using Eq. (4), we obtain the relation between the gauge-invariant phase difference and the voltage as

$$\frac{\hbar}{2e}\partial_t P_{l+1,l}(t)=\frac{\epsilon\mu^2}{sD}\left[-V_{l,l-1}(t)+\left(2+\frac{sD}{\epsilon\mu^2}\right)V_{l+1,l}(t)-V_{l+2,l+1}(t)\right]. \tag{10}$$

Note that Eq. (10) is reduced to the expression given in Eq. (7) in the limit of $\epsilon\mu^2/sD\ll1$. When we choose the values $D=6$ Å, $s=6$ Å, $\mu=2$ Å, and $\epsilon=25$ as typical parameter values for high-$T_c$ cuprates, we get $\epsilon\mu^2/D^2=2.7$. Thus we cannot neglect the correction for the Josephson relation in high-$T_c$ cuprates. The equation for the gauge-invariant phase difference, $P_{l+1,l}(t)$, is derived from Eq. (6) and the time derivative of Eq. (10) for infinite systems as

$$\frac{\epsilon}{c^2}\partial_t^2 P_{l+1,l}(t)=\frac{1}{\lambda_c^2}\left[\alpha\Delta^{(2)}\sin P_{l+1,l}(t)-\sin P_{l+1,l}(t)-\frac{\beta}{\omega_p}\partial_t P_{l+1,l}(t)+\left(\frac{I(t)}{j_c}\right)\right], \tag{11}$$

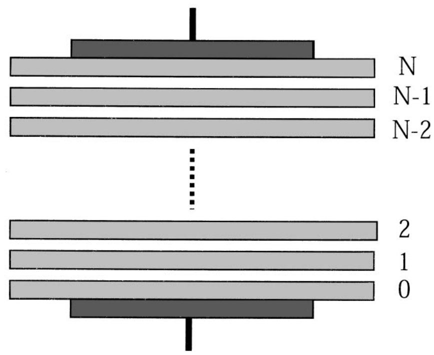


FIG. 1. A series of Josephson junctions composed of $(N+1)$ superconducting layers. The two outermost superconducting layers are contacted with electrodes.

where $\lambda_c$ is the penetration depth along the $c$ axis,

$$\lambda_c = \sqrt{c\phi_0/8\pi^2 D j_c}, \tag{12}$$

the parameters, $\alpha$ and $\beta$, are given by

$$\alpha = \frac{\epsilon\mu^2}{sD},$$

$$\beta = \frac{4\pi\sigma\lambda_c}{\sqrt{\epsilon}c}. \tag{13}$$

and $\omega_p$ is the plasma frequency, $\omega_p = c/\sqrt{\epsilon}\lambda_c$. In Eq. (11) the difference operator, $\Delta^{(2)}$, is defined as

$$\Delta^{(2)} f_{l+1,l} \equiv f_{l+2,l+1} - 2f_{l+1,l} + f_{l,l-1}. \tag{14}$$

As seen in Eq. (11), the parameter, $\alpha$, may be considered as the coupling constant between the junctions.

It is noted that Eq. (11) has a solution corresponding to the longitudinal Josephson plasma[26,27] propagating along the $c$ axis in the case of $\sigma=0$ and $I(t)=0$. Its dispersion is obtained as

$$\begin{aligned}\omega_L(k_z) &= \frac{c}{\sqrt{\epsilon}\lambda_c}\sqrt{1+2\alpha[1-\cos k_z(s+D)]}\\ &\simeq \omega_p\sqrt{1+\epsilon\mu^2[(s+D)^2/sD]k_z^2}.\end{aligned} \tag{15}$$

Since $\mu$ is very short, the dispersion of the longitudinal plasma is very weak, compared with that of the transverse one propagating along the layers, $\omega_T(\mathbf{k}) = \omega_p\sqrt{1+(\lambda_c\mathbf{k})^2}$.

To solve Eq. (11) numerically and calculate the $I$-$V$ characteristic we perform the calculations in finite systems composed of $N$ junctions in which the outermost superconducting layers ($l=0$ and $N$) are contacted with electrodes (see Fig. 1). In this case Eq. (4) for zeroth and $N$th layers is understood as follows:

$$\frac{4\pi}{\epsilon} q_0(t) = E_{1,0}(t) - E^{(-)}(t),$$

$$\frac{4\pi}{\epsilon} q_N(t) = E^{(+)}(t) - E_{N,N-1}(t), \tag{16}$$

where $q_0(t)$ and $q_N(t)$ are the total charges per unit area on zeroth and $N$th superconducting layers and $E^{(-)}(t)$ and $E^{(+)}(t)$ are the electric fields inside the electrodes. These electric fields should depend on the materials of the electrodes and the condition of the interfaces between the outermost superconducting layers and the electrodes. In the following calculations we neglect $E^{(\pm)}(t)$ for simplicity, assuming that the electrodes are well conductive, i.e., $|E^{(\pm)}(t)| \ll |E_{1,0}(t)|$, $|E_{N,N-1}(t)|$. Further we incorporate the proximity effect at the interfaces by introducing the effective width $s_0$ for zeroth and $N$th layers. Since the superconducting regions are expected to penetrate into the electrodes, we assume $s_0 > s$. Under these assumptions Eq. (16) is reduced to the following relations:

$$\frac{4\pi s_0}{\epsilon}\rho_0(t) = -E_{1,0}(t),$$

$$\frac{4\pi s_0}{\epsilon}\rho_N(t) = -E_{N,N-1}(t). \tag{17}$$

Then the equation for $P_{l+1,l}(t)$ is derived as follows:

$$\begin{aligned}\frac{\epsilon}{c^2}\partial_t^2 P_{1,0}(t) = \frac{1}{\lambda_c^2}\Bigg[&\alpha\Delta^{(1)}\sin P_{1,0}(t) - \left(1+\alpha\frac{s}{s_0}\right)\sin P_{1,0}(t)\\ &- \frac{\beta}{\omega_p}\partial_t P_{1,0}(t) + \left(\frac{I(t)}{j_c}\right)\Bigg],\end{aligned} \tag{18}$$

$$\begin{aligned}\frac{\epsilon}{c^2}\partial_t^2 P_{l+1,l}(t) = \frac{1}{\lambda_c^2}\Bigg[&\alpha\Delta^{(2)}\sin P_{l+1,l}(t) - \sin P_{l+1,l}(t)\\ &- \frac{\beta}{\omega_p}\partial_t P_{l+1,l}(t) + \left(\frac{I(t)}{j_c}\right)\Bigg],\end{aligned}$$

$$\text{for } 1 \leqslant l \leqslant N-2, \tag{19}$$

$$\begin{aligned}\frac{\epsilon}{c^2}\partial_t^2 P_{N,N-1}(t) = -\frac{1}{\lambda_c^2}\Bigg[&\alpha\Delta^{(1)}\sin P_{N-1,N-2}(t)\\ &+\left(1+\alpha\frac{s}{s_0}\right)\sin P_{N,N-1}(t)\\ &+\frac{\beta}{\omega_p}\partial_t P_{N,N-1}(t) - \left(\frac{I(t)}{j_c}\right)\Bigg],\end{aligned} \tag{20}$$

where the difference operator, $\Delta^{(1)}$, is defined as

$$\Delta^{(1)} f_{l+1,l} \equiv f_{l+2,l+1} - f_{l+1,l}. \tag{21}$$

The voltage $V_{l+1,l}(t)$ can be calculated from the following relation obtained from Eqs. (10) and (17):

$$V_{l,l-1}(t) = \frac{1}{\alpha}\frac{\hbar}{2e}\sum_{m=1}^{N}\Gamma_{lm}\partial_t P_{m,m-1}(t), \tag{22}$$

where the matrix $\Gamma = (\Gamma_{lm})$ is defined as

$$\Gamma = \Lambda^{-1}, \tag{23}$$

with

$$\Lambda=\begin{pmatrix} 1+s/s_0+\alpha^{-1} & -1 & 0 & \dots & 0 \\ -1 & 2+\alpha^{-1} & -1 & \dots & 0 \\ \vdots & \vdots & \vdots & \ddots & \vdots \\ 0 & 0 & \dots & -1 & 1+s/s_0+\alpha^{-1} \end{pmatrix} \tag{24}$$

It is noted that the current $I(t)$ in Eqs. (18)–(20) should be replaced as $I(t)\rightarrow I(t)-I_{F1}(t)$ when the effect of thermal fluctuations is incorporated in the calculations. Here, $I_{F1}(t)$ is the noise current induced in the junctions (the Johnson-Nyquist thermal noise).

The noise current is usually expressed by a random function whose spectral density is equal to $2k_BT/\pi R_N$. In the following numerical calculations we neglect the noise current for simplicity, though it becomes important as the temperature is increased. The result given in Sec. III is, thus, understood to be valid in the low temperature range near 0 K. The effect of the noise current will be discussed in a subsequent paper.

In this paper we solve the coupled equations given in (18)–(20) numerically in two cases, i.e., dc current-biased and dc voltage-biased cases. In the former case where a dc current is supplied from an external current source the current $I(t)$ in Eqs. (18)–(20) is taken to be constant, i.e., $I(t)=I$. In this case the dc voltage $V$ appearing between zeroth and $N$th layers is calculated from the relation

$$\begin{aligned}\widetilde{V}&=\lim_{T\to\infty}\frac{1}{T}\int_0^T dt\sum_{l=1}^{N}\widetilde{V}_{l,l-1}(t)\\ &=\frac{1}{\alpha}\sum_{l=1}^{N}\sum_{m=1}^{N}\Gamma_{lm}\lim_{T\to\infty}\frac{P_{m,m-1}(T)-P_{m,m-1}(0)}{T}.\end{aligned} \tag{25}$$

In the latter case where a constant voltage is applied between zeroth and $N$th layers we use the relation for $I(t)$ obtained from Eq. (6) as

$$I(t)/j_c=\frac{1}{N}\left(\beta\widetilde{V}+\sum_{l=1}^{N}\sin P_{l,l-1}(t)\right), \tag{26}$$

where $\widetilde{V}$ is the dc bias voltage in the normalized unit. The dc current in this case is calculated from the average.

$$I=\lim_{T\to\infty}\frac{1}{T}\int_0^T dt\ I(t). \tag{27}$$

## III. NUMERICAL CALCULATIONS

In this section we present the numerical results for the $I$-$V$ characteristics of 1D Josephson-junction array in the case of $N=100$ (the number of junctions is 100). The value of the parameter $\alpha$ is fixed to 2.0, which is a value in the parameter range expected in high-$T_c$ superconductors, throughout this paper.

### A. Current-biased cases

First we study the case of $s/s_0=0$. In this case the outermost superconducting layers are always neutral, i.e., $\rho_0(t)=\rho_N(t)=0$, as seen from Eq. (17), which is expected to be realized in the systems in which the mobility of the carriers between the outermost superconducting layers and the electrodes is very high. Figure 2 shows the calculated results of the $I$-$V$ characteristics for several values of $\beta$ in this case. A finite voltage appears with a sharp jump at a certain value of the bias current, which is denoted by $I_c$ from now on. The value of the current $I_c$ increases as $\beta$ increases. The behavior in the $I$-$V$ characteristics obtained in this case is qualitatively the same as that of a single Josephson junction in the current-biased case[28] (note that the McCumber constant $\beta_c$ is related to the parameter $\beta$ as $\beta_c=1/\beta^2$). In the resistive state above $I_c$ the voltage is proportional to the bias current (ohmic characteristic). To see the behavior of the gauge-invariant phase differences in this ohmic resistive state we plot $P_{l,l-1}(t)$ at three different values of time for all the junctions inside the array in Fig. 3. As seen in this figure, $P_{l+1,l}(t)$ does not show the dependence on the junction site, that is, all the gauge-invariant phase differences in this array vary in phase with time. Thus the junctions in this array behave like a single Josephson junction. Such a behavior has been observed in the $I$-$V$ characteristics of single crystals of Bi-2212 along the $c$ axis.[1,4,29]

Let us next investigate the cases of finite values of $s/s_0$. In Fig. 4 we show examples of the $I$-$V$ characteristics obtained in the cases of $s/s_0=0.5$, $\beta=0.2$ and 0.5. In both cases a small steplike structure appears in the region below the current value at which a large voltage jump appears, which is also denoted by $I_c$ in the following. In the region above $I_c$ an irregular structure is superposed on the ohmic characteristic and the irregularity increases with increasing the value of $\beta$.

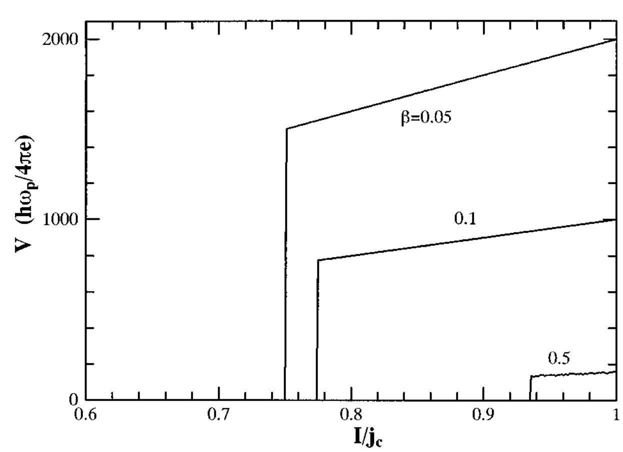


FIG. 2. $I$-$V$ characteristics of the Josephson junction array with $s/s_0=0$ in the current-biased case.

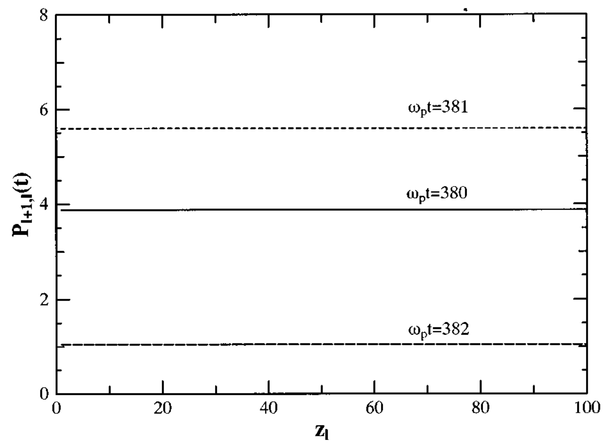


FIG. 3. Dependence of the gauge-invariant phase differences on the junction site at three different values of time in the case of $\beta=0.2$ and $s/s_0=0$. The value of the bias current is equal to $0.9j_c$.

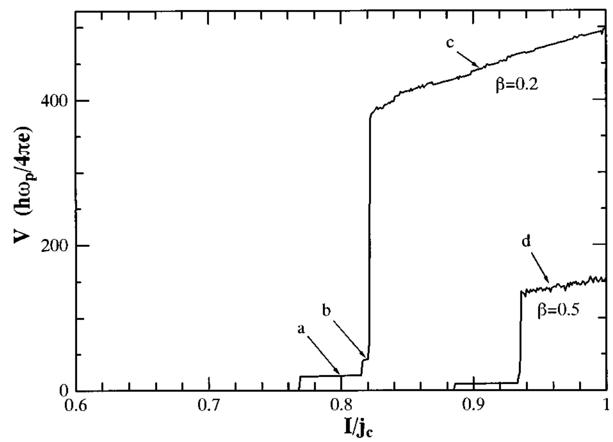


FIG. 4. $I$-$V$ characteristics of the Josephson junction array with $s/s_0=0.5$ in the current-biased case.

We first study the origin of the steplike structure appearing below $I_c$. In Figs. 5(a) and 5(b) the gauge-invariant phase differences, $P_{l+1,l}(t)$, are plotted for current values on the steps (indicated by arrows in Fig. 4) at three different values of time. As seen in these figures, only two gauge-invariant phase differences, $P_{2,1}(t)$ and $P_{99,98}(t)$ depend on time when the bias current takes a value on the first step, and for a current on the second step the gauge-invariant phase differences, $P_{2,1}(t)$, $P_{4,3}(t)$, $P_{95,94}(t)$, and $P_{99,98}(t)$ show the time

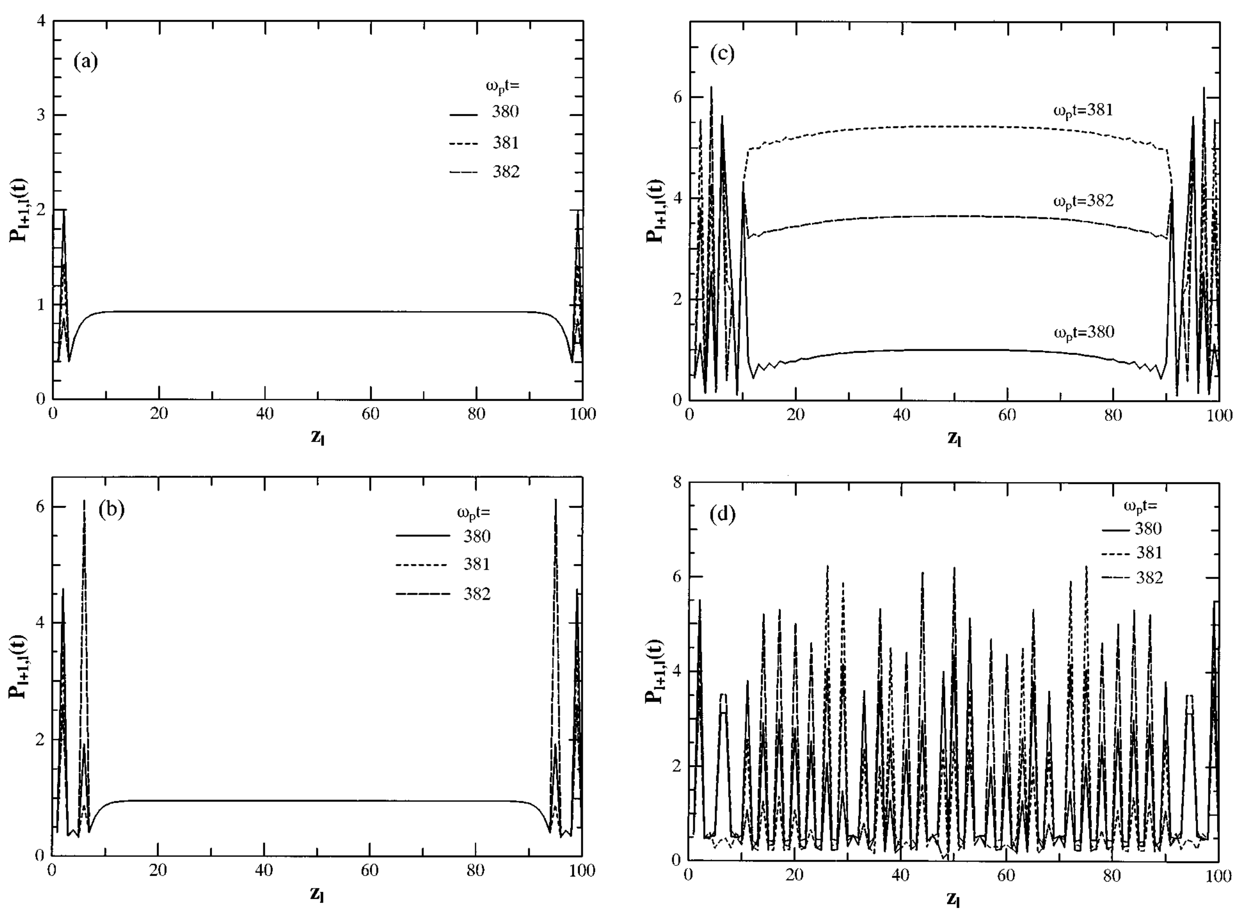


FIG. 5. (a) Dependence of the gauge-invariant phase differences on the junction site in the case of $\beta=0.2$ and $s/s_0=0.5$. The value of the bias current is equal to $0.8j_c$, which is a value on the first step in the $I$-$V$ characteristics given in Fig. 4. (b) Dependence of the gauge-invariant phase differences on the junction site in the case of $\beta=0.2$ and $s/s_0=0.5$. The value of the bias current is equal to $0.818j_c$, which is a value on the second step in the $I$-$V$ characteristics given in Fig. 4. (c) Dependence of the gauge-invariant phase differences on the junction site in the case of $\beta=0.2$ and $s/s_0=0.5$. The value of the bias current is equal to $0.9j_c$. (d) Dependence of the gauge-invariant phase differences on the junction site in the case of $\beta=0.5$ and $s/s_0=0.5$. The value of the bias current is equal to $0.96j_c$.

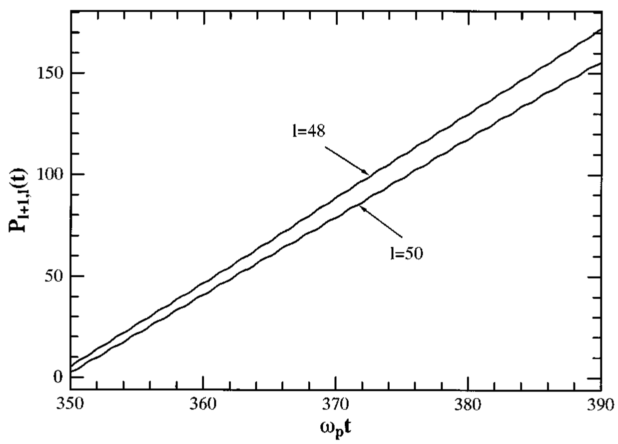


FIG. 6. Time dependence of the gauge-invariant phase differences, $P_{49,48}(t)$ and $P_{51,50}(t)$, for $I=0.96j_c$ in the Josephson junction array with $\beta=0.5$ and $s/s_0=0.5$.

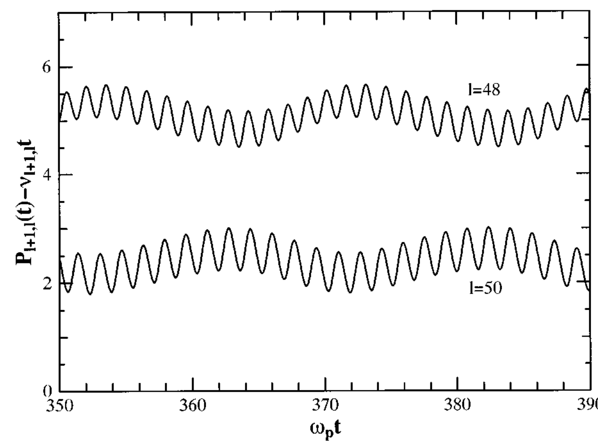


FIG. 7. Time dependence of the oscillatory terms in the gauge-invariant phase differences, $P_{49,48}(t)$ and $P_{51,50}(t)$, for $I=0.96j_c$ in the Josephson junction array with $\beta=0.5$ and $s/s_0=0.5$.

variation. This result indicates that only the junctions near the surfaces are in the resistive state and the number of such junctions increases by two at each step in this region. In recent experiments for single crystals of Bi-2212 Kadowaki *et al.* have obtained the $I$-$V$ characteristics including many small steps which is qualitatively similar to our results below the current value at which a large voltage jump takes place.[30] Although the number of steps in the $I$-$V$ characteristics shown here is very small compared with that observed in the experiments, one may expect that the steplike structure arises from the mechanism shown above, because the number of steps is expected to increase drastically for longer junction array especially in which weakly superconducting layers with smaller $j_c$ are distributed inside it, which is expected in thick samples. In Fig. 5(c) we plot $P_{l+1,l}(t)$ in the resistive state above $I_c$ in the case of $\beta=0.2$. In this case the junctions located well inside the array are also in the resistive state. It is noted that those junctions behave like a single junction, which is contrasted with the junctions located close to the surfaces. The slightly noisy voltage in the $I-V$ characteristics above $I_c$ is understood to originate from the time dependence of the gauge-invariant phase differences of the junctions near the surfaces.

Let us next investigate the system with a larger value of $\beta$ which shows much noisy $I$-$V$ characteristics ($\beta=0.5$ case in Fig. 4). The dependence of $P_{l+1,l}(t)$ on the junction site in the resistive state above $I_c$ is given in the case of $\beta=0.5$ in Fig. 5(d). The phase differences, $P_{l+1,l}(t)$, show the spatial variations with many nodes and each junction seems to behave almost independently, as seen in these figures. To understand the behavior of the phase differences in this case we study their time variations. In Fig. 6 we plot $P_{50,49}(t)$ and $P_{48,47}(t)$ as a function of time at a current value in this noisy resistive state. The time dependence of the gauge-invariant phase differences contains linear and oscillatory terms. The oscillatory terms seem to consist of mainly two frequency components, as seen in Fig. 7. The frequency of the high frequency (low) component is much larger (smaller) than the plasma frequency $\omega_p$.

Let us now study how the frequencies are determined. Extracting the linear term from the time dependence of the gauge-invariant phase difference, we express $P_{l+1,l}(t)$ as

$$P_{l+1,l}(t)=\nu_{l+1,l}t+a_{l+1,l}+\Theta_{l+1,l}(t), \tag{28}$$

where $\Theta_{l+1,l}(t)$ represents the oscillatory term. Then, Eq. (19) is rewritten in terms of the function $\Theta_{l+1,l}(t)$ as

$$\begin{aligned}\partial_t^2\Theta_{l+1,l}(t)=&\,\alpha\Delta^{(2)}\sin[\nu_{l+1,l}t+a_{l+1,l}+\Theta_{l+1,l}(t)]\\&-\sin[\nu_{l+1,l}t+a_{l+1,l}+\Theta_{l+1,l}(t)]\\&-\beta\partial_t\Theta_{l+1,l}(t)-\beta\nu_{l+1,l}+\tilde{I},\end{aligned} \tag{29}$$

with $\tilde{I}=I/j_c$. Here we use the normalized time, $\omega_p t\rightarrow t$. Since the numerical results shown above indicate that the oscillatory term is given by the sum of a high frequency component. $\Theta^{(H)}_{l+1,l}(t)$, and a low frequency one. $\Theta^{(L)}_{l+1,l}(t)$, we divide $\Theta_{l+1,l}(t)$ as $\Theta_{l+1,l}(t)=\Theta^{(H)}_{l+1,l}(t)+\Theta^{(L)}_{l+1,l}(t)$. Then the Josephson current between $l$th and $(l+1)$th layers is approximated in the following form when $\Theta^{(L)}_{l+1,l}(t)$ is small:

$$\begin{aligned}&\sin[\nu_{l+1,l}t+a_{l+1,l}+\Theta_{l+1,l}(t)]\\&\quad\simeq\sin[\nu_{l+1,l}t+a_{l+1,l}+\Theta^{(H)}_{l+1,l}(t)]\\&\quad+\cos[\nu_{l+1,l}t+a_{l+1,l}+\Theta^{(H)}_{l+1,l}(t)]\Theta^{(L)}_{l+1,l}(t).\end{aligned} \tag{30}$$

Note that the first term on the right-hand side of Eq. (30) generates a dc current if the frequency of the term $\Theta^{(H)}_{l+1,l}(t)$ coincides with $\nu_{l+1,l}$, i.e., $\Theta^{(H)}_{l+1,l}(t)=f_{l+1,l}\sin\nu_{l+1,l}t$. In this case we have the relation for the constant terms in Eq. (29),

$$\beta\nu_{l+1,l}=\tilde{I}+\Delta\tilde{I}_{l+1,l}, \tag{31}$$

where

$$\Delta\tilde{I}_{l+1,l}=J_1[f_{l+1,l}]\sin a_{l+1,l}-\alpha\Delta^{(2)}J_1[f_{l+1,l}]\sin a_{l+1,l}, \tag{32}$$

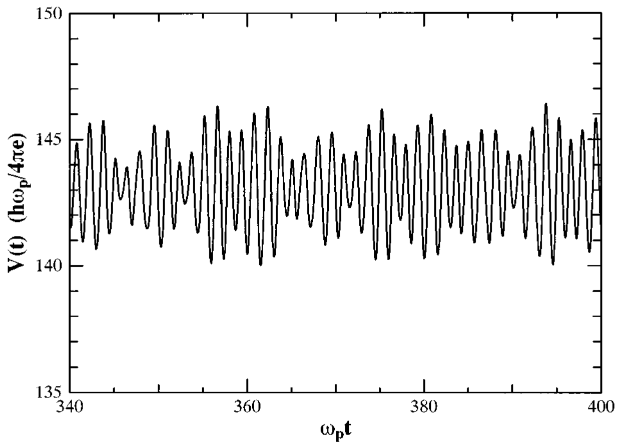


FIG. 8. Time dependence of the total voltage in the Josephson junction array with $\beta=0.5$ and $s/s_0=0.5$ for $I=0.96j_c$.

with $J_1[f_{l+1,l}]$ being the Bessel function of the first order. The numerical results shown in Figs. 6 and 7 indicates that the frequency of the term $\Theta_{l+1,l}^{(H)}(t)$ is nearly equal to the coefficient of the $t$-linear term contained in the time dependence of the gauge-invariant phase difference $P_{l+1,l}(t)$ and $\Delta\tilde{I}_{l+1,l}>0$. From these results the relation which determines the low frequency component $\Theta_{l+1,l}^{(L)}(t)$ is approximately obtained as

$$
\begin{aligned}
(\partial_t^2+\beta\partial_t)\Theta_{l+1,l}^{(L)}(t) \simeq \alpha\Delta^{(2)}\sin(\nu_{l+1,l}t+a_{l+1,l}) \\
-\sin(\nu_{l+1,l}t+a_{l+1,l}) \\
+\nu_{l+1,l}^2\sin\nu_{l+1,l}t \\
-\beta\nu_{l+1,l}\cos\nu_{l+1,l}t. \qquad (33)
\end{aligned}
$$

If the frequency $\nu_{l+1,l}$ is independent of $l$, Eq. (32) dose not have a solution oscillating with a frequency other than $\nu_{l+1,l}$. On the other hand, when $\nu_{l+1,l}$ depends on $l$ and its dependence is weak, there appears a component oscillating with a frequency much smaller than $\nu_{l+1,l}$ on the right-hand side of Eq. (33). In this case it is possible to get a solution with a frequency much less than the plasma frequency. Thus the low frequency component is understood to arise from the *beating effect* in the oscillations of the gauge-invariant phase differences. Finally we show the time dependence of the total voltage $V(t)$ appearing between zeroth and $N$th layers in Fig. 8 in this noisy resistive state. The fluctuations of the total voltage contain mainly the high frequency components. This result indicates that the motion of the low frequency mode existing in each junction is not in phase.

### B. Voltage-biased case

In the voltage-biased case we did not observe the numerical results sensitively dependent on the value of the parameter $s/s_0$. Hence we present the $I$-$V$ characteristics only in the case of $s/s_0=0$ in this paper. Figures 9(a) and 9(b) show the $I$-$V$ characteristics for $\beta=1.0$ and 0.2. As seen in these figures, very rapid oscillation of the dc current appears in the small voltage region in the case of small $\beta$ and it disappears above a certain voltage value. Since the current flowing through the junctions is carried by mainly pair electrons in the small $\beta$ case, these results suggest that the oscillation of the dc current originates from the channel of the Josephson current.

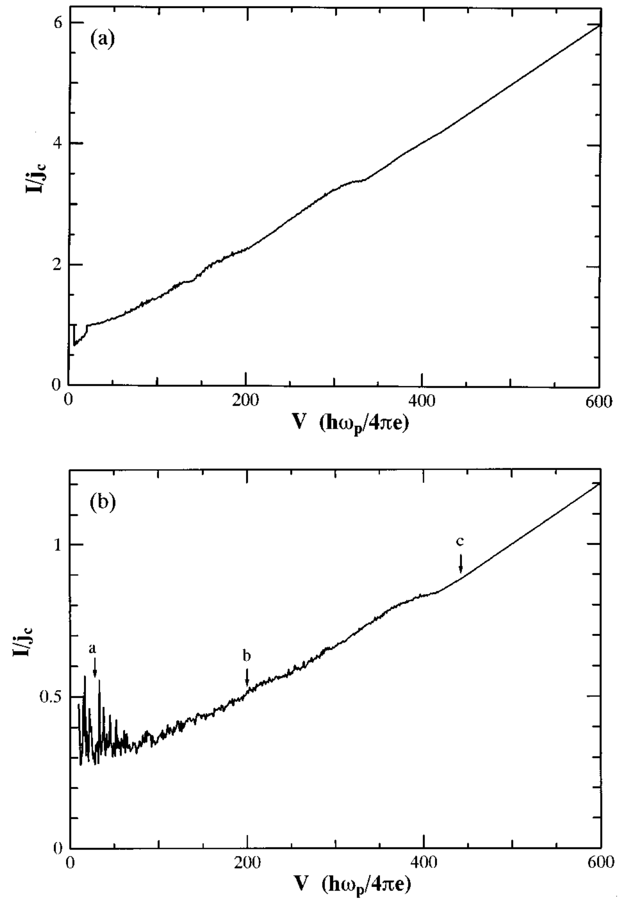


FIG. 9. (a) $I$-$V$ characteristic in the voltage-biased case in the system with the parameter values, $\beta=0.5$ and $s/s_0=0$. (b) $I$-$V$ characteristic in the voltage-biased case in the system with the parameter values, $\beta=0.2$ and $s/s_0=0$.

To clarify the origin of this noisy $I$-$V$ characteristics in the small voltage region we investigate the motion of the gauge-invariant phase differences. In Figs. 10(a)–10(c) we plot the site dependence of $P_{l+1,l}(t)$ at three different values of time for the voltage values indicated by arrows in Fig. 9(b). It is seen that the gauge-invariant phase differences show the time dependence at only certain junction sites in the small voltage case [Fig. 10(a)]. Thus the voltage takes a finite value only on those junctions in this small voltage region. The number of such junctions in the resistive state increases with increasing the applied voltage as seen in Fig. 10(b). The irregular structure in the $I$-$V$ characteristics gradually disappears with the increase of the junctions being in the resistive state. In the high voltage region without an irregular structure all the gauge-invariant phase differences vary in phase like a single junction [Fig. 10(c)]. On the basis of the results for the gauge-invariant phase differences the origin of the noisy $I$-$V$ characteristics is understood in the following way. Suppose that only certain junctions inside a Josephson junction array are in the resistive state under a weak bias voltage. The sum of the voltages on those junc-

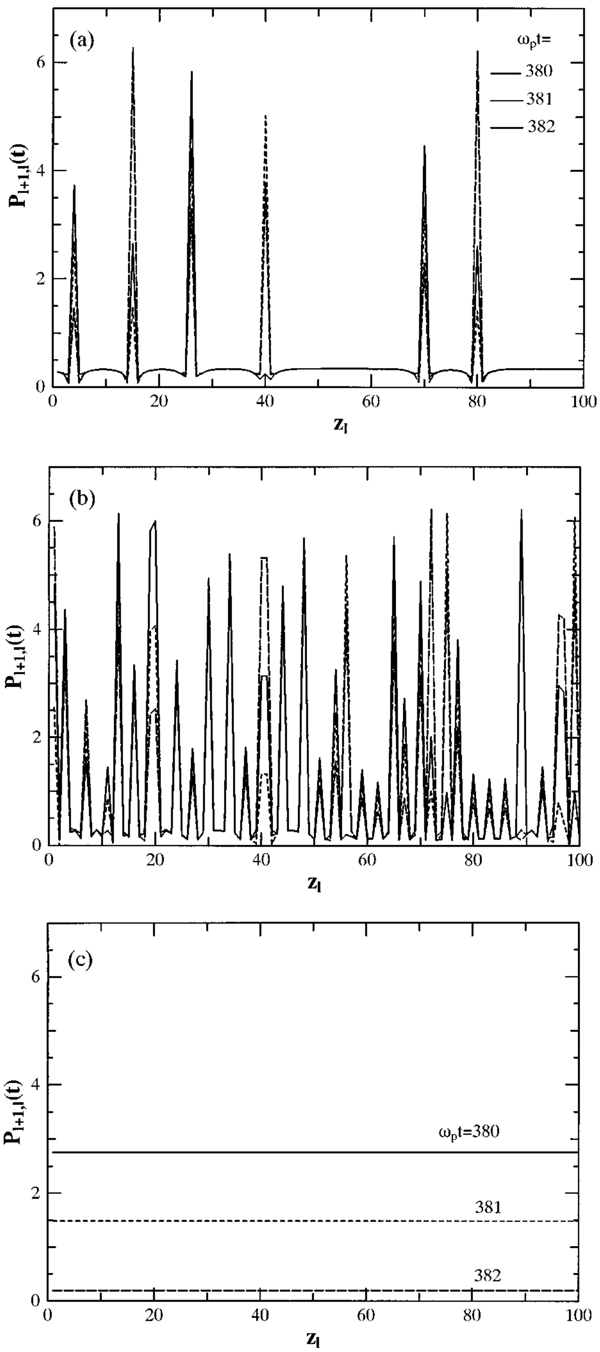


FIG. 10. (a) Dependence of the gauge-invariant phase differences on the junction site in the system with $\beta$=0.2 and $s/s_0$=0.0. The bias voltage is equal to $30\hbar\omega_p/2e$. (b) Dependence of the gauge-invariant phase differences on the junction site in the system with $\beta$=0.2 and $s/s_0$=0.0. The bias voltage is equal to $200\hbar\omega_p/2e$. (c) Dependence of the gauge-invariant phase differences on the junction site in the system with $\beta$=0.2 and $s/s_0$=0.0. The bias voltage is equal to $500\hbar\omega_p/2e$.

tions is equal to the bias voltage. Since there are a lot of ways of dividing the value of the bias voltage into the voltages on those junctions and also of choosing the junctions having finite voltages, one may expect that there exist a lot of metastable states with different voltage distribution or with the different number of junctions being in the resistive state. Furthermore it may be possible that some of such metastable states are energetically very close to the stable state. In such cases the voltage distribution inside a piece of Josephson junction array will be greatly changed with a slight variation of the bias voltage. This change may cause the rapid oscillations of the dc current.

## IV. SUMMARY

In this paper we investigated the $I$-$V$ characteristics of layered superconductors along the $c$ axis in the absence of an external magnetic field on the basis of the coupled equations derived for the gauge-invariant phase differences in 1D series of Josephson junctions. In our model the junctions in a series are coupled with each other by the charging of thin superconducting layers caused by tunneling electrons. The longitudinal plasma excitation in these systems is identified with the collective charging of the superconducting layers. Such a longitudinal mode has been observed recently in microwave absorption experiments in Bi-2212.[7,8] It has been shown that the equations for the gauge-invariant phase differences obtained in this paper have a solution corresponding to the longitudinal mode in the case without an external current.

The coupled equations for the gauge-invariant phases differences were solved numerically in both current-biased and voltage-biased cases for finite systems in which the outermost superconducting layers are contacted with electrodes. The motion of the gauge-invariant phase differences show a variety of dynamics reflecting the strong nonlinearity of the systems, depending on the intensity of the bias current or voltage and on the parameter values. The $I$-$V$ characteristics strongly reflect the dynamics of the gauge-invariant phase differences in a series.

In the current-biased case in which the charging of the two outermost superconducting layers can be neglected we have a solution corresponding to the state in which all the gauge-invariant phase differences are synchronized. In this case we have the $I$-$V$ characteristics quite similar to those of single junction systems. In the systems where the charging of the outermost superconducting layers exists there is a region of the bias current where a finite voltage appears on only certain junctions located near the electrodes. In this region a steplike structure appears in the $I$-$V$ characteristics. The number of junctions with finite voltages increases at each step.

In the voltage-biased case we have predicted that the irregular oscillations of the dc current is observed in the region of weak bias voltage in the systems where the conductivity of the quasiparticle current is small. Such a structure in the $I$-$V$ characteristics originates from a slight variation of the bias voltage causing a rapid change of the voltage distribution inside a series of the junctions.

## ACKNOWLEDGMENTS

The authors thank K. Kadowaki, H. Matsumoto, and S. Takahashi for discussions and the Materials Information Science Group for the use of the supercomputing facilities.

[1] R. Kleiner, F. Steinmeyer, G. Kunkel, and P. Müller, Phys. Rev. Lett. **68**, 2394 (1992).
[2] G. Oya, N. Aoshima, A. Irie, S. Kishida, and H. Tokutaka, J. Appl. Phys. **31**, L829 (1992).
[3] R. Kleiner and P. Müller, Phys. Rev. B **49**, 1327 (1994).
[4] P. Müller, Physica C **235–240**, 289 (1994).
[5] J. D. Hettinger, K. E. Gray, B. W. Veal, A. P. Paulikas, P. Kostic, B. R. Washburn, W. C. Tonjes, and A. C. Flewelling, Phys. Rev. Lett. **74**, 4726 (1995).
[6] S. Luo, G. Yang, and C. E. Gough, Phys. Rev. B **51**, 6655 (1995).
[7] Y. Matsuda, M. B. Gaifullin, K. Kumagai, K. Kadowaki, and T. Mochiku, Phys. Rev. Lett. **75**, 4512 (1995).
[8] O. K. C. Tsui, N. P. Ong, and J. B. Peterson, Phys. Rev. Lett. **76**, 819 (1996).
[9] See, for example, E. H. Brandt, Rep. Prog. Phys. **58**, 1465 (1995).
[10] See, for example, A. Barone and G.释ernó, *Physics and Application of the Josephson Effects* (Wiley, New York, 1982).
[11] See, for example, in *Proceedings of the Nato Advanced Research Workshop on Coherence in Superconducting Networks*, Delft, 1988, edited by J. E. Mooij and G. Schön [Physica B **152**, 1 (1988)]; H. S. J. van der Zant, H. A. Rijken, and J. E. Mooij, J. Low Temp. Phys. **79**, 289 (1990); S. P. Benz, M. S. Rzchowski, M. Tinkham, and C. J. Lobb, Phys. Rev. Lett. **64**, 693 (1990).
[12] See, for example, A. K. Jain, K. K. Likharev, J. E. Lukens, and J. E. Sauvageau, Phys. Rep. **109**, 309 (1984).
[13] P. Hadley, M. R. Beasley, and K. Wiesenfeld, Phys. Rev. B **38**, 8712 (1988).
[14] R. L. Kautz, C. A. Hamilton, and F. L. Lloid, IEEE Trans. **MAG-23**, 883 (1987).
[15] The plasma observed in the microwave experiments using $TE_{102}$ cavity mode by Matsuda *et al.* (Ref. 7) is understood to be the longitudinal one. This result suggests that the charging of the superconducting layers takes place even in the microwave region.
[16] W. Lawrence and S. Doniach, in *Proceeding of the 12th International Conference on Low Temperature Physics*, edited by E. Kanda (Keigaku, Tokyo, 1971), p. 361.
[17] T. Koyama, N. Takezawa, and M. Tachiki, Physica C **172**, 501 (1991).
[18] L. N. Bulaevskii and J. R. Clem, Phys. Rev. B **44**, 10 234 (1991).
[19] S. Sakai, P. Bodin, and N. F. Pedersen, J. Appl. Phys. **73**, 2411 (1993).
[20] L. N. Bulaevskii, M. Zamora, D. Baeriswyl, H. Beck, and J. R. Clem, Phys. Rev. B **50**, 12 831 (1994).
[21] The dispersion of the plasma mode given in Eq. (13) in Ref. 20 is not correct, because the wave number dependence along the *c* axis vanishes for the plasma propagating in the direction parallel to the *c* axis.
[22] B. D. Josephson, Adv. Phys. **14**, 419 (1965).
[23] P. W. Anderson and A. H. Dayem, Phys. Rev. Lett. **13**, 195 (1964).
[24] H. Suhl, Phys. Rev. Lett. **14**, 226 (1965).
[25] H. Umezawa, H. Matsumoto, and M. Tachiki, *Thermo Field Dynamics and Condensed States* (North-Holland, Amsterdam, 1982).
[26] M. Tachiki, T. Koyama, and S. Takahashi, Phys. Rev. B **50**, 7065 (1994): in *Coherence in High Temperature Superconductors*, edited by G. Deutsher and A. Revolevschi (World Scientific, Singapore, 1996), p. 371.
[27] T. Koyama and M. Tachiki, Solid State Commun. **96**, 386 (1995).
[28] D. M. McCumber, J. Appl. Phys. **39**, 3113 (1968).
[29] A. Yurgens, D. Winkler, Y. M. Zhang, N. Zavaritsky, and T. Claeson, Physica C **235–240**, 3269 (1994).
[30] K. Kadowaki, T. Mochiku, H. Takeya, K. Hirata, and Y. Saito, Physica C **235–240**, 3275 (1994).